BIOCHEMISTRY
including biophysical chemistry & molecular biology

Article

pubs.acs.org/biochemistry

Mutational Analysis of Divalent Metal Ion Binding in the Active Site of Class II α-Mannosidase from *Sulfolobus solfataricus*

Dennis K. Hansen,[†] Helen Webb,[†] Jonas Willum Nielsen,[†] Pernille Harris,[‡] Jakob R. Winther,[†] and Martin Willemoës*[,†]

[†]Section for Biomolecular Sciences, Department of Biology, University of Copenhagen, Ole Maaløes Vej 5, DK-2200 Copenhagen, Denmark

[‡]Department of Chemistry, Technical University of Denmark, Building 206, DK2800 Kgs. Lyngby, Denmark

ABSTRACT: Mutational analysis of *Sulfolobus solfataricus* class II α-mannosidase was focused on side chains that interact with the hydroxyls of the −1 mannosyl of the substrate (Asp-534) or form ligands to the active site divalent metal ion (His-228 and His-533) judged from crystal structures of homologous enzymes. D534A and D534N appeared to be completely inactive. When compared to the wild-type enzyme, the mutant enzymes in general showed only small changes in K_M for the substrate, *p*-nitrophenyl-α-mannoside, but elevated activation constants, K_A, for the divalent metal ion (Co^{2+}, Zn^{2+}, Mn^{2+}, or Cd^{2+}). Some mutant enzyme forms displayed an altered preference for the metal ion compared to that of the wild type-enzyme. Furthermore, the H228Q, H533E, and H533Q enzymes were inhibited at increasing Zn^{2+} concentrations. The catalytic rate was reduced for all enzymes compared to that of the wild-type enzyme, although less dramatically with some activating metal ions. No major differences in the pH dependence between wild-type and mutant enzymes were found in the presence of different metal ions. The pH optimum was 5, but enzyme instability was observed at pH <4.5; therefore, only the basic limb of the bell-shaped pH profile was analyzed.

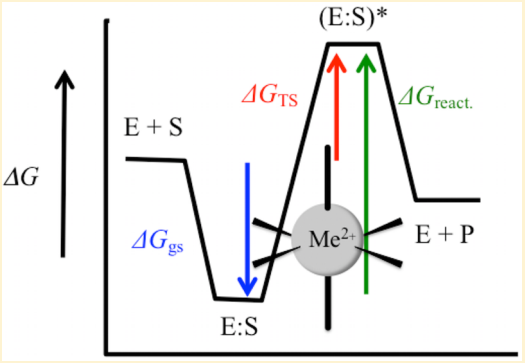

The class II α-mannosidase (GH38) is characterized by a divalent metal ion forming a platform in the active site that assists in binding the mannosyl at position −1 preceding the scissile bond.[1−3] We have previously characterized the substrate specificity of ManA, a GH38 member from the crenarchaeon *Sulfolobus solfataricus*, with respect to the steady state kinetics of glycosidic bond cleavage in the enzyme prepared with a range of catalytically competent divalent metal ions.[4] Mammals and other eukaryotes possess three isozymes located in the cytosol, the Golgi, and lysosomes.[5,6] The crystal structure of the bovine lysosomal enzyme[7] and the *Drosophila melanogaster* Golgi enzyme[8,9] serve as the basis for a structural understanding of these two isozymes. The mammalian enzymes cleave a subset of the α-1,2, α-1,3, and α-1,6 glycosidic bonds of various mannobioses or larger mannose structures.[10,11] Bacterial and archaeal enzymes in addition also cleave α-1,4 mannosidic bonds,[12,13] and in this respect, *S. solfataricus* ManA resembles these enzymes.[4,14] However, we and others have shown that this promiscuity toward the glycosidic bond depends greatly on the metal ion complexed in the active site.[4,14] For *S. solfataricus* ManA, only Co^{2+} facilitated the cleavage of the α-1,6 bond in mannobioses and only Mn^{2+} supported catalytic efficiencies for α-1,2 and α-1,4 bonds that were comparable to those obtained with Co^{2+}.[4] Also, for the artificial substrate, pNP-mannoside, the highest catalytic efficiency was observed in the presence of Co^{2+}.[4] These observations together with those of others[13] opposed the generally accepted notion that class II α-mannosidases are Zn^{2+}-containing enzymes as also originally shown to be the case for *S. solfataricus* ManA.[14]

The side chains that coordinate the active site divalent metal ion and/or interact with the mannosyl moiety preceding the scissile bond are all fully conserved among known GH38 enzymes (Figure 1A). Two histidines and two aspartic acid residues (Figure 1B) bind the metal ion.[1,15,16] The two remaining ligands in the T_6-octahedral coordination sphere of the divalent metal ion are constituted by the 2- and 3-hydroxyls of the terminal −1 mannosyl moiety of the substrate.[1] In the absence of substrate in the active site, the coordination sphere of the bound metal ion is T_5-square-based pyramidal with the four mentioned side chains and a single water molecule as ligands.[9,15] Of the two aspartyls complexing the metal ion, one is also the nucleophile in the otherwise classical catalytic machinery of the glycosidase retaining mechanism.[1]

The divalent metal ion bound to the active site is a prerequisite for binding of the substrate. ManA treated with EDTA has no detectable activity, and the steady state kinetic mechanism is ordered with metal ion binding first and then substrate.[4] However, the metal ion participates in binding the terminal mannosyl at the −1 position and promotes catalysis by

Received: January 29, 2015
Revised: March 5, 2015
Published: March 9, 2015

DOI: 10.1021/acs.biochem.5b00090
Biochemistry 2015, 54, 2032−2039

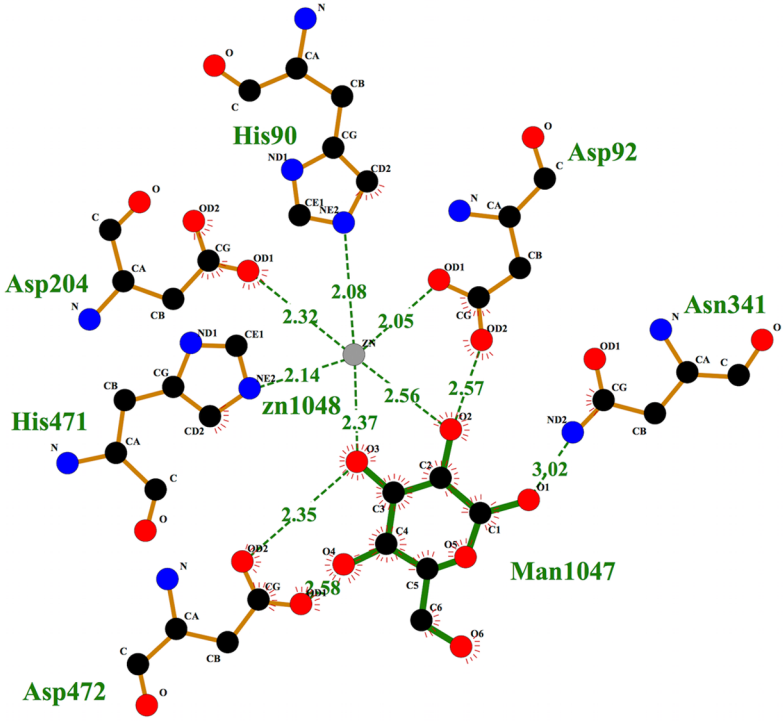

Figure 1. Representation of the active site residues of *D. melanogaster* class II α-mannosidase and their interaction with Zn^{2+} and mannose. The numbering of residues is for the *D. melanogaster* enzyme, which corresponds to the following residues in *S. solfataricus*: His-228 (His-90), Asp-230 (Asp-92), His-533 (His-471), Asp-534 (Asp-472), and Asp-338 (Asp-204). The acid/base in *S. solfataricus* ManA (corresponding to Asp-341, replaced by Asn in the structure) is not readily identified on the basis of protein sequence alignment. The figure was drawn using Protein Data Bank entry 3bup in LigPlot.[20]

distorting the ring structure of this mannosyl in the transition state,[7,15,16] and it has been implicated in stabilizing the buildup of a negative charge on the mannosyl O1 and the partial deprotonation of the 2-hydroxyl during glycosidic bond cleavage in quantum mechanics/molecular mechanics (QM/MM) simulations.[3] Other side chains that interact directly with the mannosyl are a tyrosine and an aspartyl (Tyr-727 and Asp-472, respectively, in the *D. melanogaster* enzyme) that form hydrogen bonds with the 4-hydroxyl and the 3- and 4-hydroxyls, respectively.

In this work, *S. solfataricus* ManA served as a template for the analysis of the role in substrate binding, metal ion binding, catalysis, and the pH profile of the two histidines, His-228 and His-533 (His-90 and His-471, respectively, in the *D. melanogaster* enzyme), which constitute two of the four ligands to the metal ion, and the carboxylate Asp-534 (Asp-471 in the *D. melanogaster* enzyme), which interacts directly with the −1 mannosyl 3- and 4-hydroxyls. Although an exchange of the side chains that interact with the divalent metal ion can be predicted to greatly affect the binding of this, our work indicates that altered electrostatics that follow from this side chain exchange also greatly impact the catalytic efficiency of the enzyme. The mutational analysis described in this work provides experimental data to improve our understanding of the unusual active site of GH38 class II α-mannosidases compared to other glycosidases by encompassing a divalent metal ion.

EXPERIMENTAL PROCEDURES

Construction of Mutant Alleles and Protein Purification. The mutant *S. solfataricus* ManA-encoding alleles were constructed by the polymerase chain reaction (PCR) megaprimer method combining mutagenic primers as listed below in combination with primers 166:5′-GTGAGCGGATAACAATTCCCCTC-3′ and 167:5′-GCAGCCAACTCAGCTTCCTTTCGG-3′. The latter two primers anneal to the template JWN01 in regions outside the ManA encoding part of the plasmid. The pJWN01 plasmid is a pET11a derivative with the *S. solfataricus* ManA reading frame inserted between the NdeI and BamHI restriction sites as described previously.[4] For the megaprimer synthesis, primer 166 was combined with mutagenic primers labeled at the 5′ end and primer 167 was combined with mutagenic primers labeled at the 3′ end. The mutagenic primers were as follows: H228E5′, 5′-CTGGTCACGCT**GAG**ATTGATACCGC-3′; H228E3′, 5′-GCGGTATCAAT**CTC**AGCGTGACCAG-3′; H228Q5′, 5′-GGTCACGCTCA**G**ATTGATACCGCTTGG-3′; H228Q3′, 5′-CCAAGCGGTATCAAT**C**TGAGCGTGACC-3′; H533E5′, 5′-GGATCAGTTC**GAA**GACGTCTTACC-3′; H533E3′, 5′-GGTAAGACGTC**TTC**GAACTGATCC-3′; H533E5′, 5′-GATCAGTTCCA**GG**ACGTCTTACC-3′; H533E3′, 5′-GGTAAGACGTC**C**TGGAACTGATC-3′; D534N5′, 5′-CAGTTCCAT**A**ACGTCTTACCTGGATCG-3′; D534N3′, 5′-CGATCCAGGTAAGACGT**T**ATGGAACTG-3′; D534A5′, 5′-CAGTTCCATG**C**CGTCTTACCTGGATCG-3′; D534A3′, 5′-CGATCCAGGTAAGACG**G**CATGGAACTG-3′. Bold lettering corresponds to introduced mutations. Double mutations were constructed by using the relevant single-mutation allele as a template for the PCRs. The products from fusion of relevant megaprimers were cloned into the NdeI and BamHI restriction sites in pET11a and verified by sequencing of the entire coding region.

Protein purification was performed as previously described.[4] Briefly, cells of *Escherichia coli* strain BL21(DE3) harboring the pRARE plasmid (Rosetta), pJWN01, or the relevant mutant

DOI: 10.1021/acs.biochem.5b00090
Biochemistry 2015, 54, 2032−2039

Table 1. Kinetic Parameters Obtained by Varying pNP-Mannoside in the Presence of the Indicated Divalent Metal Ions for *S. solfataricus* Wild Type and Mutant Class II α-Mannosidases[a]

enzyme	divalent metal ion	k_{cat} (s^{-1})	$k_{cat,comp.A}$ (s^{-1})	K_M (mM)	k_{cat}/K_M[b] (mM^{-1} s^{-1})
WT	Co^{2+}	11.3 ± 0.4		0.35 ± 0.04	32.3
	Zn^{2+}	6.6 ± 0.2		0.74 ± 0.06	8.9
	Mn^{2+}	4.8 ± 0.2		0.47 ± 0.06	10.2
	Cd^{2+}	15.3 ± 0.7		1.9 ± 0.2	8.1
H228E	Co^{2+}	0.80 ± 0.04	0.99	1.4 ± 0.2	0.57 (0.70)
	Zn^{2+}	0.118 ± 0.006		1.1 ± 0.2	0.11
	Mn^{2+}	*c*		*c*	0.019 ± 0.009
	Cd^{2+}	1.18 ± 0.07		2.7 ± 0.4	0.43
H228Q	Co^{2+}	1.6 ± 0.1	2.3	1.7 ± 0.3	0.94 (1.35)
	Zn^{2+}	0.60 ± 0.06		2.5 ± 0.6	0.24
	Mn^{2+}	*c*		*c*	0.038 ± 0.001
	Cd^{2+}	*c*		*c*	0.53 ± 0.02
H533E	Co^{2+}	4.3 ± 0.1		2.9 ± 0.2	1.5
	Zn^{2+}	*c*		*c*	0.0732 ± 0.0004
	$Zn^{2+,d}$	*c*		*c*	0.240 ± 0.005
	Mn^{2+}	*c*		*c*	0.014 ± 0.002
	Cd^{2+}	*c*		*c*	0.046 ± 0.001
H533Q	Co^{2+}	0.099 ± 0.003		0.13 ± 0.02	0.76
	Zn^{2+}	1.42 ± 0.05		1.9 ± 0.2	0.75
	$Zn^{2+,c}$	1.6 ± 0.1		1.1 ± 0.2	1.5
	Mn^{2+}	0.088 ± 0.005		0.7 ± 0.1	0.13
	Cd^{2+}	0.40 ± 0.02		1.1 ± 0.2	0.36

[a]Assay conditions and data analysis were as described in Experimental Procedures. [b]Values in parentheses are calculated on the basis of $k_{cat,comp.A}$. [c]K_M was too high (≥10 mM for pNP-Man or ≥0.1 mM for Mn^{2+}) to allow for determination of kinetic parameters other than k_{cat}/K_M. [d]Metal ion concentration of 0.1 mM.

derivative of pJWN01 were grown in 2 L of a phosphate-buffered salt medium supplemented with tryptone and yeast extract[17] and the addition of chloramphenicol (50 μg/mL) and ampicillin (500 μg/mL) to maintain plasmids. At an OD_{436} of 8−10, protein synthesis was induced with 1 mM IPTG and growth continued overnight. Cells were washed twice in 50 mM potassium phosphate (pH 7.5), resuspended in sonication buffer [50 mM Tris-HCl (pH 8.0)], and disrupted by sonication, and insoluble matter was removed by centrifugation. As observed previously,[4] >90% of wild-type and mutant protein remained in the pellet with insoluble material. To the supernatant was added streptomycin sulfate to a concentration of 1%, and the supernatant was cleared by centrifugation. The supernatant was heated to 80 °C for 20 min and cleared by centrifugation. To the supernatant from the heating step was added ammonium sulfate to 80% saturation, and the pellet recovered by centrifugation was dissolved in 50 mM Tris-HCl (pH 8.0), dialyzed against the same buffer, loaded on a 5 mL HiTrap Q (GE healthcare) anion exchange column equilibrated with 50 mM Tris-HCl (pH 8.0), and eluted by a NaCl gradient from 0 to 0.5 M over 6 column volumes. Fractions containing the enzyme as evaluated by sodium dodecyl sulfate−polyacrylamide gel electrophoresis were pooled and loaded directly on a 5 mL HiTrap Phenyl FF (GE Healthcare) hydrophobic interaction column. The column was washed with 25 mM Tris-HCl (pH 8.0) and 0.5 M NaCl and eluted with a gradient from wash buffer to pure water over 5 column volumes. The fractions containing enzyme with a purity of approximately ≥95% were collected by 80% saturated ammonium sulfate precipitation and subsequent centrifugation, and the pellet was redissolved in 3 mL of 50 mM Tris-HCl (pH 8.0). The apoenzyme was prepared by incubation in 50 mM Tris-HCl (pH 8.0) and 5 mM EDTA at 70 °C for 1 h followed by successive dialysis twice in 200 mL of 50 mM Tris-HCl (pH 8.0) and 5 mM EDTA followed by three stages of dialysis against 200 mL of 50 mM Tris-HCl (pH 8.0). The apoenzyme was stored at 4 °C. The procedure described above yielded approximately 2−3 mg of soluble mutant or wild-type enzyme.

Kinetic Analysis of Wild-Type and Mutant ManA Enzymes. All assays were performed at 70 °C in assay buffer [45 mM acetate (pH 5.0)] unless otherwise stated. The concentrations of pNP-mannoside and the chloride salt of divalent metal ions were fixed at 4.5 and 1 mM, respectively, in the standard assay or varied in the ranges from 0 to 10 mM and from 0 to 1 mM, respectively, depending on the kinetic parameters, except for the fact that the Mn^{2+} concentration did not exceed 0.1 mM as this ion alone promotes substantial hydrolysis of pNP-mannoside above this concentration. One hundred microliter samples of assay mix in 500 μL PCR tubes were transferred to a PCR machine. Because *S. solfataricus* ManA is essentially inactive at temperatures below 30 °C, the reaction was initiated in the PCR machine by the temperature increase from 4 to 70 °C and stopped by the cooling to 4 °C after incubation for 40 min. To the reaction mixtures was added 200 μL of 1 M sodium carbonate, to dissociate all the released pNP for quantification at 410 nm after transfer of 200 μL aliquots to a 96-well tray. Initial rates were determined at least twice at different enzyme concentrations. The pH optima for wild-type and mutant enzymes in the presence of 1 mM metal ion (0.1 mM for Mn^{2+}), as listed under Results, and 4.5 mM pNP-mannoside were determined by replacing the assay buffer described above with 45 mM succinate adjusted to maintain the respective pH at 70 °C, as shown in Results. To investigate the stability of wild-type ManA with varying pH, the enzyme dissolved in 50 mM Tris-HCl (pH 8) with the addition of 1 mM $CoCl_2$ was diluted 1:3 in 200 mM succinate buffer with the

DOI: 10.1021/acs.biochem.5b00090
Biochemistry 2015, 54, 2032−2039

Table 2. Kinetic Parameters for Divalent Metal Ion Activation of pNP-Mannoside Hydrolysis for *S. solfataricus* Wild-Type and Mutant Class II α-Mannosidases[a]

enzyme	divalent metal ion	k_{cat} (s^{-1})	$k_{cat,comp.S}$ (s^{-1})	K_A (μM)	k_{cat}/K_A[b] (μM^{-1} s^{-1})
WT	Co^{2+}	10.2 ± 0.3	11.0	0.7 ± 0.1	14.6 (15.7)
	Zn^{2+}	6.0 ± 0.3	6.98	0.8 ± 0.3	7.5 (8.7)
	Mn^{2+}	3.5 ± 0.2	3.9	0.6 ± 0.2	5.8 (6.5)
	Cd^{2+}	9.3 ± 0.2	13.2	0.20 ± 0.03	46.5 (66.0)
H228E	Co^{2+}	0.77 ± 0.02	1.01	236 ± 16	0.0033 (0.0042)
	Zn^{2+}	0.146 ± 0.002	0.182	17 ± 2	0.0085 (0.0107)
	Mn^{2+}	[c]		[c]	[c]
	Cd^{2+}	0.76 ± 0.02	1.22	77 ± 6	0.0099 (0.0158)
H228Q	Co^{2+}	1.3 ± 0.1	1.8	439 ± 105	0.0030 (0.0041)
	Zn^{2+}	0.8 ± 0.1[d]		105 ± 35[d]	0.008
	Mn^{2+}	[c]		[c]	[c]
	Cd^{2+}	2.9 ± 0.1		180 ± 27	0.016
H533E	Co^{2+}	2.24 ± 0.01	4.76	70 ± 1	0.032 (0.068)
	Zn^{2+}	1.21 ± 0.07[c]		9 ± 5[c]	0.121
	Mn^{2+}	[e]		[e]	0.0051 ± 0.0001
	Cd^{2+}	0.269 ± 0.003		11 ± 2	0.024
H533Q	Co^{2+}	0.076 ± 0.003	0.108	7 ± 2	0.010 (0.015)
	Zn^{2+}	1.80 ± 0.08[d]		3.3 ± 0.9[d]	0.55
	Mn^{2+}	0.107 ± 0.003	0.124	8.3 ± 0.9	0.013 (0.015)
	Cd^{2+}	0.294 ± 0.006	0.366	5.7 ± 0.7	0.052 (0.064)

[a]Assay conditions and data analysis were as described in Experimental Procedures. [b]Values in parentheses are calculated on the basis of $k_{cat,comp.S}$. [c]K_A was too high to allow for determination of kinetic parameters other than k_{cat}/K_A. [d]Data were fit to eq 2: K_I = 0.7 ± 0.3 mM for H228Q, K_I = 0.49 ± 0.04 mM for H533E, and K_I = 1.0 ± 0.2 mM for H533Q. [e]Activity could not be reliably determined at metal ion concentrations below 50 μM.

pH varying from 3 to 7. The pHs of the end solutions was confirmed by mixing 50 mM Tris-HCl (pH 8) with succinate buffers to record the true final pH of the mixed solution. The enzyme mixed with succinate buffer was then incubated at 70 °C for 40 min when it was diluted a further 4-fold in 50 mM Tris-HCl (pH 8) and assayed for activity by the standard procedure described above in the presence of 1 mM $CoCl_2$ as the activating metal ion.

Data from determination of initial rates were analyzed using the following equations to obtain the kinetic parameters listed under results: eq 1 for hyperbolic substrate or activator saturation (for the latter case, see the explanation below), eq 2 for data that revealed the occurrence of activator inhibition, and eq 3 for analyzing data from varying pHs. Equations 4 and 5 were used to calculate k_{cat} when the kinetic data for substrate or divalent metal ion were available, in the case where these were subsaturating in experiments where the other component was varied as described in Results. Equation 6 is the Eyring–Polanyi equation for calculating the change in Gibbs free energy of transition state formation for the substrate or the activator (for the latter case, see the explanation below). Equation 7 calculates the Gibss free energy change difference between wild-type and mutant enzymes.

$$v = \frac{k_{cat}[S]}{K_M + [S]} \quad (1)$$

$$v = \frac{k_{cat}[A]}{K_A + [A] + \frac{[A]^2}{K_I}} \quad (2)$$

$$v = \frac{v_{opt}}{1 + \frac{10^{-pK_a}}{10^{-pH}}} \quad (3)$$

$$k_{cat,comp.A} = \left(\frac{[S]_{fixed}}{[S]_{fixed} + K_M}\right)^{-1} k_{cat} \quad (4)$$

$$k_{cat,comp.S} = \left(\frac{[A]_{fixed}}{[A]_{fixed} + K_A}\right)^{-1} k_{cat} \quad (5)$$

$$\Delta G^{\ddagger} = -RT \ln\left(\frac{h \times k_{cat}/K_M}{K_A T}\right) \quad (6)$$

$$\Delta\Delta G^{\ddagger}_{Mut-WT} = \Delta G^{\ddagger}_{Mut} - \Delta G^{\ddagger}_{WT} \quad (7)$$

where v is the initial rate and k_{cat} is the apparent maximal rate at infinite concentrations of the varied substrate, S, or activating divalent metal ion, A, that then replaces S in eq 1. K_M is the apparent Michaelis–Menten constant for the substrate, S, replaced by K_A when A is varied. K_I is the inhibition constant for A at increasing concentrations. v_{opt} is the initial rate at the optimal pH, and pK_a is the value determined for the activity of the enzyme. $k_{cat,comp.}$ is the value of k_{cat} compensated for the reduced activity arising from a limiting fixed concentration of substrate or activator (i.e., ~10-fold less than the Michaelis–Menten constant, K_M or K_A). $\Delta G^{\ddagger}$ is the Gibbs free energy of transition state formation calculated from k_{cat}/K_M in the case where pNP-mannoside is varied (Table 1) or replaced by k_{cat}/K_A when the activating metal ion was varied (Table 2). k_{cat} was replaced by $k_{cat,comp.}$ when the latter is given in Tables 1 and 2. h and k_B are the Planck and Boltzmann constants, respectively. For $\Delta G^{\ddagger}_{Mut}$ and $\Delta G^{\ddagger}_{WT}$, the suffix Mut refers to the mutant enzyme and WT refers to wild-type ManA.

RESULTS

Protein Production and Purification. All mutant enzymes were, like the wild type, produced as ~95% insoluble protein.[4] The soluble fraction of each mutant enzyme was

DOI: 10.1021/acs.biochem.5b00090
Biochemistry 2015, 54, 2032–2039

similar to that of the wild type. Similar activity in the presence of Co^{2+} for wild-type and mutant enzymes was obtained when they were tested before and after the EDTA treatment that involves incubating the protein at 70 °C for 1 h (Experimental Procedures). We therefore conclude that the mutant enzymes have maintained a structural integrity in terms of thermostability similar to that of the wild-type enzyme.

Kinetic Analysis of pNP-Mannoside Hydrolysis by Wild-Type and Mutant ManA's in the Presence of Various Divalent Metal Ions. Double-mutant enzymes H228Q/H533Q and H228E/H533E and single-mutant enzymes D534Q and D534A showed no detectable activity (k_{cat} < 0.01 s^{-1}) within the pH range of 3−7 and with Co^{2+} as the activating divalent metal ion and were therefore not investigated further.

For the remaining active mutant enzymes and the wild-type enzyme, we determined the kinetic parameters for pNP-mannoside hydrolysis in the presence of a fixed concentration of Co^{2+}, Zn^{2+}, Mn^{2+}, and Cd^{2+} (Table 1) and the kinetic parameters for divalent metal ion activation in the presence of a fixed pNP-mannoside concentration (Table 2) as described in Experimental Procedures. It should be noted that this approach produces only apparent kinetic constants, and k_{cat} values may vary between Tables 1 and 2. This is mainly because the fixed pNP-mannoside concentration in many cases was limiting because of a dramatically increased K_M for some mutant enzymes. However, where a high K_M for pNP-mannoside (>0.5 mM) was observed, we were not able saturate these enzymes because of the moderate solubility of the substrate. This means that some k_{cat} values in Tables 1 and 2 are underestimated, and in an attempt to compensate for this flaw, we have used eqs 4 and 5 to calculate $k_{cat,comp.}$ that takes into account the unsaturation of the enzyme with respect to substrate, or in a few cases, the divalent metal ion as listed in Tables 1 and 2. However, it should be stressed that this compensation does not take into account the full complexity correlating the kinetic constants for binding of substrate and divalent metal ion in the ordered sequential binding mechanism established for ManA.[4]

All four divalent metal ions activate the wild-type enzyme, and their relative efficiency in activating the pNP-mannoside hydrolysis reaction as determined by the specificity constant, k_{cat}/K_M, has previously been documented.[4] Co^{2+} is by far the most efficient metal ion in stimulating pNP-mannoside hydrolysis, 3−4-fold better when compared to the other metal ions. Previous observations[4] correlate well with those made in this work (Table 1), although the K_M values determined here in general, by comparison, appear to be slightly increased.

For the H228E enzyme, the main difference in the kinetic parameters for pNP-mannoside hydrolysis compared to those of the wild-type enzyme was a k_{cat} lowered by ∼10−15-fold in the presence of Co^{2+} and Cd^{2+} but ∼65-fold in the presence of Zn^{2+} (Table 1). The Mn^{2+}-catalyzed reaction was greatly impaired, and only k_{cat}/K_M could be determined for this reaction, which was 600-fold lower than for the wild-type enzyme (Table 1). The kinetic parameters for metal ion activation of the H228E enzyme showed a decrease in k_{cat} consistent with that for pNP-mannoside saturation (Table 2). In contrast to the K_M values for pNP-mannoside, the K_A for Co^{2+} and Cd^{2+} had increased 300−400-fold but only ∼20-fold for Zn^{2+}. The K_A for Mn^{2+} could not be reliably determined as the activity of the enzyme in the presence of this ion was too low in combination with the fact that Mn^{2+} for technical reasons had to be kept below 0.1 mM in the assay (Experimental Procedures).

The kinetic parameters for pNP-mannoside hydrolysis by the H228Q enzyme in the presence of Co^{2+}, Zn^{2+}, and Mn^{2+} were quite similar to those of the H228E enzyme (Table 1). In the presence of Cd^{2+} though, the K_M was too high to be determined but the k_{cat}/K_M was in the same range as for the H228E enzyme. The kinetic parameters for metal ion activation of H228Q also showed increases in K_A of orders of magnitude compared to that of the wild-type enzyme, and k_{cat}/K_A values similar to that of H228E for both enzymes displayed decreases of 1000−5000-fold (Table 2). However, in contrast to H228E, but like H533E and H533Q presented below, the H228Q enzyme showed inhibition at increasing concentrations of Zn^{2+} with a K_I ∼7-fold higher than K_A (Table 2).

The H533E enzyme showed >10-fold increases in K_M for pNP-mannoside, and only in the presence of Co^{2+} was it possible to determine the individual kinetic parameters, K_M and k_{cat} (Table 1). Clearly, Co^{2+} is the preferred metal ion in pNP-mannoside hydrolysis for H533E with only a 20-fold reduced k_{cat}/K_M compared to 100-, 1000-, and 200-fold decreases in k_{cat}/K_M in the presence of Zn^{2+}, Mn^{2+}, and Cd^{2+}, respectively, when compared to that of wild-type ManA (Table 1). In the case of Zn^{2+}, reducing the concentration of this ion 10-fold to 0.1 mM increased the k_{cat}/K_M of H533E for pNP-mannoside 3-fold (Table1), probably by eliminating part of the inhibition observed at higher concentrations of this ion (see below). The k_{cat}/K_A values for Co^{2+}, Zn^{2+}, and Cd^{2+} obtained with the H533E enzyme were quite similar within a 5-fold range (Table 2). For Mn^{2+}, the k_{cat}/K_M was 5−6-fold lower than that observed for Co^{2+} and Cd^{2+} and 20-fold lower than that for activation by Zn^{2+} (Table 2).

In contrast to the H553E enzyme, the H533Q enzyme showed K_M values similar to that of the wild-type enzyme, so that the reduced values of k_{cat}/K_M observed for pNP-mannoside hydrolysis by this mutant enzyme were mainly caused by reductions in k_{cat} of ∼100-, ∼50-, and 40-fold for the Co^{2+}-, Mn^{2+}-, and Cd^{2+}-activated reactions, respectively (Table 1). With Zn^{2+}, however, k_{cat} was lowered only 4-fold for the H533Q enzyme, making this the preferred metal ion also in terms of k_{cat}/K_M for pNP-mannoside, although Zn^{2+} also inhibited the H533Q enzyme (Table 2) primarily by increasing the K_M for pNP-mannoside as is indicated by comparing the kinetic parameters obtained at 1 or 0.1 mM Zn^{2+} in the assay (Table 1). The K_A values determined for the H533Q enzyme were very similar for all four metal ions (Table 2), but k_{cat} was 6-fold higher with Zn^{2+} than with Cd^{2+}, which in turn was 3−4 times higher than that with Co^{2+} and Mn^{2+} (Table 2).

We also tested if the change in the side chains in mutant enzymes H228Q, H228E, H533Q, and H533E induced the ability of using other divalent, or trivalent, metal ions that do not activate the wild-type enzyme. The mutant enzymes were incubated in the presence of 4.5 mM pNP-mannoside and 1 mM $NiCl_2$, $CuCl_2$, $AlCl_3$, or $FeCl_3$, but in no case did we detect any activity above background levels.

Determination of pH Optima for Wild-Type and Mutant ManA. The pH dependence of wild-type *S. solfataricus* ManA in the presence of Co^{2+} showed a very steep increase in activity coming from the acidic side of the pH optimum. In fact, the pH profile was found to be very narrow, and the optimum was found to be 5.0 (Figure 2). The shape of the pH profile indicated that the increase in activity at acidic pH was not derived from simple titration of a side chain in the active site,

DOI: 10.1021/acs.biochem.5b00090
Biochemistry 2015, 54, 2032−2039

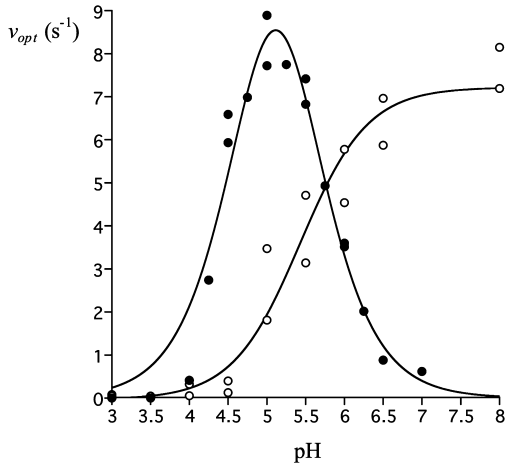

Figure 2. Activity and stability of wild-type ManA as a function of pH in the presence of Co^{2+}. Experiments were performed as describesd in Experimental Procedures. Stability (○) of ManA determined at pH 5.0 after incubation at the indicated pH for 40 min. Activity (●) of ManA determined at the indicated pH. The uppermost (basic) pK_a for the enzyme activity profile was 5.3 ± 0.2, and the pK_a for the enzyme stability curve was 5.4 ± 0.1. Experiments were performed as described in Experimental Procedures.

and we therefore performed an analysis of the stability of the enzyme in the investigated pH interval. From Figure 2, it is clear that the stability of ManA is greatly dependent on pH. The enzyme is completely inactivated upon being incubated under the conditions described in Experimental Procedures and exposed to a pH ≤4.5. This dramatically complicates the analysis of the pH optimum because the enzyme activity, with an apparent optimum at pH 5.0, drops more than 10-fold in contrast to enzyme stability that increases when the solution approaches pH 8.0. However, to compare the pH profiles of wild-type and mutant enzymes, we also determined the enzyme activity of the mutant enzymes in the interval from pH 3 to 7. These experiments (data not shown) showed that all the enzymes, regardless of the activating divalent metal ion, had an optimum around pH 5.0. Therefore, the only meaningful analysis of the pH-dependent activity response of wild-type and mutant enzymes appeared to be an estimate of the pK_a value for the basic side of the bell-shaped pH optimum. The calculated pK_a values are listed in Table 3. Note that because H228Q, H533E, and H533Q are inhibited in the presence of Zn^{2+} as indicated in Table 2 and the activity of the mutant enzymes in the presence of Mn^{2+} generally was too low to provide meaningful data, these metal ions were not tested with these enzymes.

The only significant differences between wild-type and mutant enzymes in Table 3 are the lower pK_a values observed for H533E in the presence of Cd^{2+} and for H533Q in the presence of Co^{2+} or Cd^{2+}. This decrease in pK_a, however, does not really seem to correlate with changes in the kinetic parameters of pNP-mannoside hydrolysis (Table 1) or metal ion activation (Table 2).

DISCUSSION

Apart from verification of the catalytic residues, the nucleophile, and the general acid/base,[1,9,11] no mutational studies of class II α-mannosidase enzymes have been performed so far, despite the unusual architecture of the active site that involves a divalent metal ion interacting directly with the nucleophile and

Table 3. pK_a Values Calculated from Data Covering the Basic Part of the Bell-Shaped pH Optimum (pH range of 5−7) for *S. solfataricus* Wild-Type and Mutant Class II α-Mannosidases[a]

enzyme	divalent metal ion	v_{opt} (s^{-1})	pK_a
WT	Co^{2+}	10.9 ± 0.7	5.67 ± 0.07
	Zn^{2+}	6.3 ± 1.2	5.8 ± 0.3
	Mn^{2+}	5.9 ± 0.2	6.29 ± 0.05
	Cd^{2+}	12.3 ± 0.8	5.60 ± 0.08
H228E	Co^{2+}	0.67 ± 0.09	5.7 ± 0.2
	Cd^{2+}	0.92 ± 0.2	5.8 ± 0.2
H228Q	Co^{2+}	0.5 ± 0.1	5.9 ± 0.3
	Cd^{2+}	0.9 ± 0.3	5.8 ± 0.5
H533E	Co^{2+}	2.8 ± 0.3	5.7 ± 0.2
	Cd^{2+}	0.5 ± 0.2	5.0 ± 0.2
H533Q	Co^{2+}	0.16 ± 0.02	5.3 ± 0.1
	Cd^{2+}	0.6 ± 0.1	5.3 ± 0.2

[a]Experiments were performed and the parameters derived using eq 3 as described in Experimental Procedures.

serving as a binding platform for the −1 mannosyl moiety to be cleaved from the substrate. The highly conserved side chains at positions 228, 533, and 534 in *S. solfataricus* ManA are shown to interact with either the divalent metal ion or the substrate in crystal structures of homologues enzymes.[1,7,15] This work represents the first characterization of mutant class II α-mannosidase enzymes altered in the divalent metal ion binding site.

Three mutant enzymes, H228Q, H533E, and H533Q, were all inhibited by high Zn^{2+} concentrations (Table 2). The simplest explanation for this phenomenon may be that the active site in these mutant enzymes can accommodate an additional Zn^{2+} that hinders the binding of pNP-mannoside in the active site or prevents catalysis. One may speculate that inhibition with Zn^{2+} and not any of the other tested divalent metal ions is a result of Zn^{2+} willingly entering a tetrahedral coordination sphere in proteins,[18] and therefore, two ions can be accommodated in the mutant binding sites. In the wild-type enzyme, this site is optimized for a pentacoordinated square pyramidal (no ligand) or hexacoordinated octahedral (bound ligand) complex.[9,15]

No dramatic differences in the fold decrease in activity from that of the wild-type enzyme with an increasing pH were observed for the mutant enzymes. However, the calculated pK_a values from data of varying pH (Table 3) are obviously rather complex and composed of more than just a titration of side chains in the active site, as indicated by the results from the analysis of the wild-type enzyme with respect to stability and activity with varying pH (Figure 2).

The D534A and D534N enzymes showed no detectable activity under standard conditions outlined in Experimental Procedures. However, Asp-534, by analogy to the crystal structure of other class II α-mannosidases, interacts with the 3- and 4-hydroxyls of the −1 mannosyl[1,3,7,15] but because of the lack of activity appears to fulfill more than a simple binding function. If Asp-534 interacts with only substrate in the ground state, we consider it more likely that the change in the side chain at position 534 would result in mainly an elevated K_M. We speculate that Asp-534 plays a crucial catalytic role by fixing the O2−C2−C3−O3 bonds of the −1 mannosyl and thereby assisting in converting the conformation of the $^4C_1$ pyranose into the ground state $^0S_2/B_{2,5}$ intermediate complex and further

DOI: 10.1021/acs.biochem.5b00090
Biochemistry 2015, 54, 2032−2039

into the $B_{2,5}$ conformation in the transition state to end with the skew boat conformation ($^1S_5$) in the covalent intermediate as suggested from QM/MM calculations.[3] Similarly positioned carboxylates (Asp-348, Bt3990) are also found in the inverting Ca^{2+}-dependent α-mannosidases, GH92.[19]

It was evident from our previous kinetic analysis of ManA,[4] where the active site metal ion had been systematically removed and replaced by Co^{2+}, Mn^{2+}, Cd^{2+}, Zn^{2+}, Ni^{2+}, and Cu^{2+}, that the two latter metal ions do not support activity and the first four do so in such a manner that kinetic parameters for hydrolysis of pNP-mannoside and various mannobioses changed markedly depending on which activating metal ion was included in the assay.[4] The efficiency of a divalent metal ion in activating ManA is probably a result of the ion's ability, via its coordination sphere, to stabilize the pyranose conformation of the −1 mannosyl and introduce the high-energy tension during transition state formation.[3,16] Compared to the wild-type enzyme, we do not observe dramatic changes for mutant enzymes H228E, H228Q, and H533Q in the K_M for pNP-mannoside, except in the presence of Mn^{2+} for H228E and H228Q or Cd^{2+} for the H533Q enzyme (Table 1 and Figure 3A). The overall trend for these mutant enzymes seems

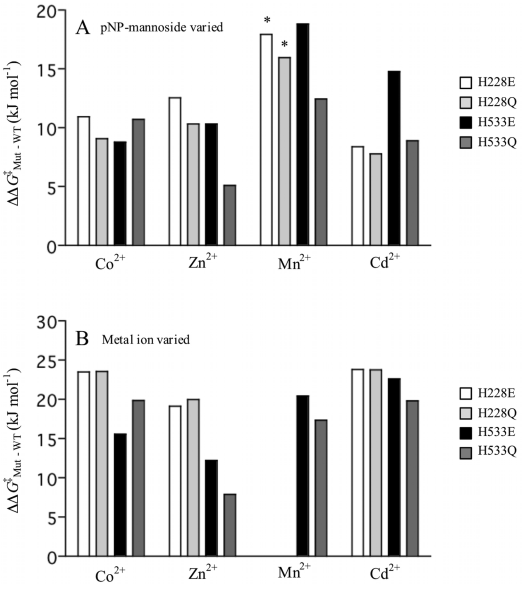

Figure 3. Values of $\Delta\Delta G^{\ddagger}_{Mut-WT}$ for (A) varying pNP-mannoside and (B) varying the activating divalent metal ion. The activating metal ion present in the assay is indicated on the *X*-axis, and the coloring of bars according to the mutant enzyme is shown. An asterisk indicates that this condition is greatly unsaturated with divalent metal ion as explained in Results. Experiments were performed as outlined in Experimental Procedures and the footnotes of Tables 1 and 2.

to be that they are mainly affected in the binding of the metal ion as indicated by the increase in K_A from 20-fold to more than several orders of magnitude (Table 2 and Figure 3B), when compared to that of the wild-type enzyme. Thus, it is the increase in K_A for the mutant enzymes that gives dramatically lower values for k_{cat}/K_A than for k_{cat}/K_M compared to those of the wild-type enzyme (Tables 1 and 2 and Figure 3). The effect of the side chain alterations in H228E, H228Q, and H533Q, which also varies depending on the metal ion, on kinetic parameters reflects the importance of the same side chains in binding the metal ion and situating it correctly in the transition state.[3,16]

For the H533E enzyme, however, the picture is a bit more complex. We were able to determine the K_M for pNP-mannoside only in the presence of Co^{2+}, which also proved to be by far the best divalent metal ion for this enzyme to stimulate the reaction (Table 1). The kinetic properties of the H533E enzyme seemed to demonstrate, by immeasurably high K_M values, that a carboxylate in place of His-533 greatly hampered binding of the substrate, whereas the K_A for Co^{2+}, Zn^{2+}, and Cd^{2+} did not change dramatically compared to those of the enzymes altered at position 228 or the H533Q enzyme. That H533E and H533Q have so markedly different kinetic properties compared to the more similar H228E and H228Q enzymes may in the case of H533E be ascribed to a problem of accommodating a negative charge so close to three other carboxylates: the nucleophile, the general acid/base, and Asp-534 [Asp-204, Asp-341, and Asp-472 in the *D. melanogaster* enzyme (Figure 1)].[1,7,15] Introducing a fourth carboxylate is likely to interfere with the binding network involving the carboxylates already present, the metal ion, and the substrate mannosyl (Figure 1) and obstruct substrate binding.

A QM/MM analysis of the reaction path for class II α-mannosidase based on crystal structures of the *D. melanogaster* enzyme[3] suggests that Asp-92 (Asp-230 in *S. solfataricus* ManA) plays a key role in catalysis by facilitating a partial proton transfer from the 2-hydroxyl of the substrate −1 mannosyl to Asp-92. A concomitant buildup of negative charge on the O2 atom as the hydrogen is approaching Asp-92 is stabilized by the active site divalent metal ion, and we conclude that the interaction between O2 and Zn^{2+} is important for catalysis.

As mentioned in the introductory section and discussed above, the divalent metal ion has also been implicated in distorting the ring structure of the −1 mannosyl to facilitate formation of the transition state.[7,15,16] A similar function in catalysis has been proposed for the Ca^{2+} ion in GH92 mannosidases.[19] Interestingly, mutant enzymes of GH92, where the side chains involved in binding Ca^{2+} have been changed to alanyl, give rise to similar changes in kinetic properties compared to those of the wild-type enzyme as we observe for the H228E, H228Q, and H533Q enzymes with moderate changes in K_M for the substrate and a 10−100-fold decrease in k_{cat}.[19]

In conclusion, the data in this work support the role of the metal ion in formation of the transition state in ManA. The side chains at positions 228 and 533 are obviously involved in binding the activating metal ion as their primary function. This was also evident from published structures of the enzyme.[1,7,15] However, the fact that the metal ion plays such a dramatic role in transition state formation as originally suggested from computational analysis[3] is also greatly supported by our observations here. Although no detail could be obtained for the inactive mutant proteins D534A and D534N, it is clear from our work that Asp-534 fulfills a crucial role in catalysis that cannot be described by only contributing to simple binding of substrate.

AUTHOR INFORMATION

Corresponding Author

*Phone: +45 3532 2030. E-mail: willemoes@bio.ku.dk.

Funding

This work was supported by the Danish Council for Independent Research, Technology and Production Sciences.

DOI: 10.1021/acs.biochem.5b00090
Biochemistry 2015, 54, 2032−2039

Notes

The authors declare no competing financial interest.

■ ACKNOWLEDGMENTS

We acknowledge the expert technical assistance by Aida Curovic.

■ ABBREVIATIONS

Mutant enzymes are abbreviated according to the position of the changed residue, e.g., H228E means that His-228 is changed to glutamyl in that enzyme; pNP, *p*-nitrophenolate; pNP-mannoside, *p*-nitrophenyl-α-mannoside.

■ REFERENCES

(1) Numao, S., Kuntz, D. A., Withers, S. G., and Rose, D. R. (2003) Insights into the mechanism of *Drosophila melanogaster* Golgi α-mannosidase II through the structural analysis of covalent reaction intermediates. *J. Biol. Chem. 278*, 48074−48083.

(2) Shah, N., Kuntz, D. A., and Rose, D. R. (2008) Golgi α-mannosidase II cleaves two sugars sequentially in the same catalytic site. *Proc. Natl. Acad. Sci. U.S.A. 105*, 9570−9575.

(3) Petersen, L., Ardevol, A., Rovira, C., and Reilly, P. J. (2010) Molecular mechanism of the glycosylation step catalyzed by Golgi α-mannosidase II: A QM/MM metadynamics investigation. *J. Am. Chem. Soc. 132*, 8291−8300.

(4) Nielsen, J. W., Poulsen, N. R., Johnsson, A., Winther, J. R., Stipp, S. L., and Willemoes, M. (2012) Metal ion dependent catalytic properties of *Sulfolobus solfataricus* class II α-mannosidase. *Biochemistry 51*, 8039−8046.

(5) Opheim, D. J., and Touster, O. (1978) Lysosomal α-D-mannosidase of rat liver. Purification and comparison with the golgi and cytosolic α-D-mannosidases. *J. Biol. Chem. 253*, 1017−1023.

(6) Haeuw, J. F., Michalski, J. C., Strecker, G., Spik, G., and Montreuil, J. (1991) Cytosolic glycosidases: Do they exist? *Glycobiology 1*, 487−492.

(7) Heikinheimo, P., Helland, R., Leiros, H. K., Leiros, I., Karlsen, S., Evjen, G., Ravelli, R., Schoehn, G., Ruigrok, R., Tollersrud, O. K., McSweeney, S., and Hough, E. (2003) The structure of bovine lysosomal α-mannosidase suggests a novel mechanism for low-pH activation. *J. Mol. Biol. 327*, 631−644.

(8) Rose, D. R. (2012) Structure, mechanism and inhibition of Golgi α-mannosidase II. *Curr. Opin. Struct. Biol. 22*, 558−562.

(9) van den Elsen, J. M., Kuntz, D. A., and Rose, D. R. (2001) Structure of Golgi α-mannosidase II: A target for inhibition of growth and metastasis of cancer cells. *EMBO J. 20*, 3008−3017.

(10) Moremen, K. W., Ernst, B., Hart, G. W., and Sinaý, P. (2008) α-Mannosidases in Asparagine-Linked Oligosaccharide Processing and Catabolism. In *Carbohydrates in Chemistry and Biology*, pp 81−117, Wiley-VCH Verlag GmbH: Berlin.

(11) Zhong, W., Kuntz, D. A., Ember, B., Singh, H., Moremen, K. W., Rose, D. R., and Boons, G. J. (2008) Probing the substrate specificity of Golgi α-mannosidase II by use of synthetic oligosaccharides and a catalytic nucleophile mutant. *J. Am. Chem. Soc. 130*, 8975−8983.

(12) Wong-Madden, S. T., and Landry, D. (1995) Purification and characterization of novel glycosidases from the bacterial genus *Xanthomonas*. *Glycobiology 5*, 19−28.

(13) Angelov, A., Putyrski, M., and Liebl, W. (2006) Molecular and biochemical characterization of α-glucosidase and α-mannosidase and their clustered genes from the thermoacidophilic archaeon *Picrophilus torridus*. *J. Bacteriol. 188*, 7123−7131.

(14) Cobucci-Ponzano, B., Conte, F., Strazzulli, A., Capasso, C., Fiume, I., Pocsfalvi, G., Rossi, M., and Moracci, M. (2010) The molecular characterization of a novel GH38 α-mannosidase from the crenarchaeon *Sulfolobus solfataricus* revealed its ability in de-mannosylating glycoproteins. *Biochimie 92*, 1895−1907.

(15) Suits, M. D., Zhu, Y., Taylor, E. J., Walton, J., Zechel, D. L., Gilbert, H. J., and Davies, G. J. (2010) Structure and kinetic investigation of *Streptococcus pyogenes* family GH38 α-mannosidase. *PLoS One 5*, e9006.

(16) Kuntz, D. A., Liu, H. Z., Bols, M., and Rose, D. R. (2006) The role of the active site Zn in the catalytic mechanism of the GH38 Golgi α-mannosidase II: Implications from noeuromycin inhibition. *Biocatal. Biotransform. 24*, 55−61.

(17) Lauritsen, I., Willemoes, M., Jensen, K. F., Johansson, E., and Harris, P. (2011) Structure of the dimeric form of CTP synthase from *Sulfolobus solfataricus*. *Acta Crystallogr. F67*, 201−208.

(18) Rulisek, L., and Vondrasek, J. (1998) Coordination geometries of selected transition metal ions (Co^{2+}, Ni^{2+}, Cu^{2+}, Zn^{2+}, Cd^{2+}, and Hg^{2+}) in metalloproteins. *J. Inorg. Biochem. 71*, 115−127.

(19) Zhu, Y., Suits, M. D., Thompson, A. J., Chavan, S., Dinev, Z., Dumon, C., Smith, N., Moremen, K. W., Xiang, Y., Siriwardena, A., Williams, S. J., Gilbert, H. J., and Davies, G. J. (2010) Mechanistic insights into a Ca^{2+}-dependent family of α-mannosidases in a human gut symbiont. *Nat. Chem. Biol. 6*, 125−132.

(20) Wallace, A. C., Laskowski, R. A., and Thornton, J. M. (1995) LIGPLOT: A program to generate schematic diagrams of protein-ligand interactions. *Protein Eng. 8*, 127−134.

DOI: 10.1021/acs.biochem.5b00090
Biochemistry 2015, 54, 2032−2039